

# The relation between far-UV and visible extinctions.

Frédéric Zagury

02210 *Saint Rémy Blanzy, France* <sup>1</sup>

---

## Abstract

For directions of sufficient reddening ( $E(B - V) > \sim 0.25$ ), there is a simple relation between the slope of the extinction curve in the far-UV and  $E(B - V)$ . Regardless of direction, the far-UV extinction curve is proportional to  $1/\lambda^n e^{-2E(B-V)/\lambda}$  ( $\lambda$  in  $\mu\text{m}$ ,  $n = 4$ ), in accordance with the idea that reddened stars spectra are contaminated by scattered light (Zagury, 2001b).

This relation is not compatible with the standard theory of extinction which states that far-UV and visible extinctions are due to different classes of grains. In that model the two (far-UV and visible) extinctions vary thus independently according to the proportion of each type of grains.

In preceding papers I have shown that the standard theory cannot explain UV observations of nebulae, and is contradicted by the UV spectra of stars with very low reddening: for how long shall the standard theory be considered as the interpretation of the extinction curve?

*Key words:* ISM: Dust, extinction

*PACS:* 98.38.j, 98.38.Cp, 98.58.Ca

---

## 1 Introduction

Extinction curves normalized by  $E(B - V)$  are similar in the visible part of the spectrum, but they exhibit noticeable differences in the far-UV (Savage et al., 1985).

If the light we receive from a reddened star is only direct starlight, as it is supposed by the standard theory of extinction, the optical and the far-UV extinctions must be caused by different types of grains. The important

---

<sup>1</sup> E-mail: fzagury@wanadoo.fr

variations observed in the far-UV slope of the normalized extinction curves are due to the different proportions of each type of grain from one region to another.

I have shown in a previous series of papers the possibility for the far-UV light that we receive from the direction of a reddened star, to be mainly light scattered at small angular distances from the star and re-injected into the beam of the observation. The phase lag between two trajectories of the scattered light is smaller than UV wavelengths if the scattering particles are inside a small cone (angle less than  $\sim 10^{-7}''$ , which encompasses a few 100 A.U. for a cloud distant of 100 pc, Zagury (2001b)) centered on the star. If scattering is due to particles small enough to have equal reflectance, then the scattering is coherent and the intensity of the scattered light is -unless multiple scattering is important- proportional to the square of the number of particles within the cone.

One important consequence of this interpretation is that the linear visible extinction of starlight extends to the UV. This was verified up to the bump region for stars with not too high reddening ( $E(B-V) \leq 0.5$ , Zagury (2000b)), for which scattered light is important in the far-UV only.

In the far-UV, scattering is enhanced because extinction, and the number of photons available for scattering, is higher. Coherent scattering considerably amplifies the intensity of the scattered light, which - assuming a linear extinction law in the far-UV- can reach around 20 % of the direct starlight corrected for extinction (Zagury, 2000b). This is by far larger than the reddened direct starlight if extinction is important. For example,  $E(B-V) \sim 0.5$  yields a ratio at  $\lambda = 1500 \text{ \AA}$  of scattered light to direct starlight of  $\sim 0.2/e^{-2E(B-V)/\lambda} = 160$  ( $\lambda$  in  $\mu\text{m}$ , see Zagury (2000b)). Of course, if extinction is large, either because  $E(B-V)$  is large or towards the shortest wavelengths, scattered light is finally extinguished, as direct starlight is.

For large enough  $E(B-V)$  the far-UV light we receive from a star is nearly all scattered light. If scattered light is extinguished like direct starlight as  $e^{-2E(B-V)/\lambda}$ , and since the scattering cross section of the small particles varies as  $1/\lambda^n$  ( $n \geq 4$ , Jackson (1975)), we expect the spectrum of the scattered light -and the far-UV spectrum of a star with sufficient reddening- to vary as  $\lambda^{-n}e^{-2E(B-V)/\lambda}$  (Zagury, 2001a). We see that the slope of the far-UV extinction curve is now related to the slope of its' optical part.

In this framework, the reduced spectrum of a reddened star (the spectrum of the star divided by the spectrum of an unreddened star of same spectral type, Zagury (2000b)) multiplied by  $\lambda^n$  must be an exponential; the exponent determines the far-UV slope of the reduced spectrum, independently of the exact value of  $n$ .  $n = 4$ , the Rayleigh scattering case, gave a good fit to the

spectrum of HD46223 (Zagury, 2001a) and is adopted hereafter.

The idea of this paper is to take stars with sufficient reddening, and to study the dependence on  $\lambda$  of their far-UV reduced spectrum multiplied by  $\lambda^4$ . The product is expected to decrease exponentially. Determination of the exponent  $E_{uv}$  gives an estimate of  $E(B - V)$ .  $E_{uv}$  can be compared to the value,  $E_{vis}$ , found for  $E(B - V)$  from the spectral type of the star and its' optical color  $B - V$ . I expect  $E_{uv}$  and  $E_{vis}$  to have close values. Possible contamination of direct starlight by scattered light in the visible will give an observed color of a star which underestimates the exact  $B - V$  (Zagury, 2001a). It implies that  $E_{vis}$  can be slightly smaller than  $E_{uv}$  (Zagury, 2001a). The exact value of  $E(B - V)$  is given by  $E_{uv}$ .

Section 2 presents the data. The determination of  $E(B - V)$  from the far-UV spectra and the comparison with the values derived from the optical properties of the stars is made in section 3. The result is discussed in section 4. A summary is given in the conclusion.

## 2 Data

The stars of Table 1 correspond to a wide range of different extinction curves and reddenings. These stars belong to existing atlases of extinction curves (Savage et al., 1985; Fitzpatrick & Massa, 1990; Aiello et al., 1988) that I have used in the past three years. Stars with too low reddening ( $E(B - V) < \sim 0.2 - 0.3$ ) are not suitable to the purpose of the paper: for these stars direct starlight is not negligible in the UV and the reddening of the comparison stars becomes an important source of uncertainty. They have been discarded.

Some particular objects, like the Red Rectangle, were not included. The current comprehension of the Red Rectangle (Waelkens et al., 1995), is that HD44179 is hidden behind a thick disk of interstellar matter; we do not receive direct starlight from the direction of the star but only light scattered from the poles of the disc.

The far-UV spectra were retrieved from the IUE database (<http://iuearc.vilspa.esa.es>). For each star an unreddened star of close spectral type was found and used to obtain the reduced spectra. The numbers in column 7 of Table 1 refer to the comparison star number of Table 2.

$B - V$  comes from SIMBAD database (<http://simbad.u-strasbg.fr>). In general these values agree with Tycho satellite estimates (also available at SIMBAD), after multiplication by  $\sim 0.92$  to take into account the difference of Tycho and Johnson filters.

### 3 Data analysis

The far-UV reduced spectra, multiplied by  $\lambda^4$  are plotted, figure 1 to figure 3, with an arbitrary scaling factor along the y-axis (logarithm y-coordinate). Comparison stars have been corrected for the extinction in their direction, as indicated in Zagury (2001c). This correction is e.g. smaller or of the same order than the uncertainty on  $E_{uv}$  and cannot affect the results of the paper.

The resulting spectra decrease exponentially in the far-UV (figures 1 to 3). The exponent  $2E_{uv}$  is written after the number of the star and reported in the sixth column of Table 1.

Figure 4 plots  $2E_{uv}$  versus  $2E_{vis}$ . This figure has three main sources of uncertainty.

A first source of error is a possible mismatch on the spectral type of the stars, and/or a difference between the spectral types of the star and of the comparison star. Except for an improbable large mistake on the spectral type, the value of  $2E_{vis}$  will not be altered too much. But, spectral type mismatch can noticeably change the slope  $2E_{uv}$  of the reduced spectrum of the star. For Cardelli & Savage (1988) HD62542 is a B5V. If the star is a B3V (Houk, 1978), the cross representing HD62542 on figure 4 will be shifted up by 0.3 mag.. These errors are discussed in several papers (Bless & Savage, 1972; Nandy et al., 1975). They can represent a few 0.1 mag., but they are difficult to quantify. They are not included in the error margin given for  $2E_{uv}$  (Table 1).

The error on  $2E_{uv}$  given in Table 1 corresponds to the uncertainty once a spectral type is adopted. For the stars with the largest reddening (figure 3), the increasing importance of the 2200 Å bump on the long wavelength side, and the Ly $\alpha$  emission on the short wavelength side of the spectrum, render difficult a precise determination of the slope. Consequently, the uncertainty on  $2E_{uv}$  is increased.

Last, some objects are special. For the Red Rectangle (discarded here, section 2),  $E(B - V)$  determined from the visible magnitudes has no meaning at all, because the star is hidden behind a huge amount of interstellar matter and is not directly observed. Particular objects should in general be stars embedded in dust clouds.

Although these sources of error can occasionally modify figure 1 to figure 4, the general conclusions I would derive from the examination of these figures are:

- Between the 2200 Å bump and the Ly $\alpha$  region the (far-UV reduced spectrum) $\times\lambda^4$  product can be assimilated to an exponential.

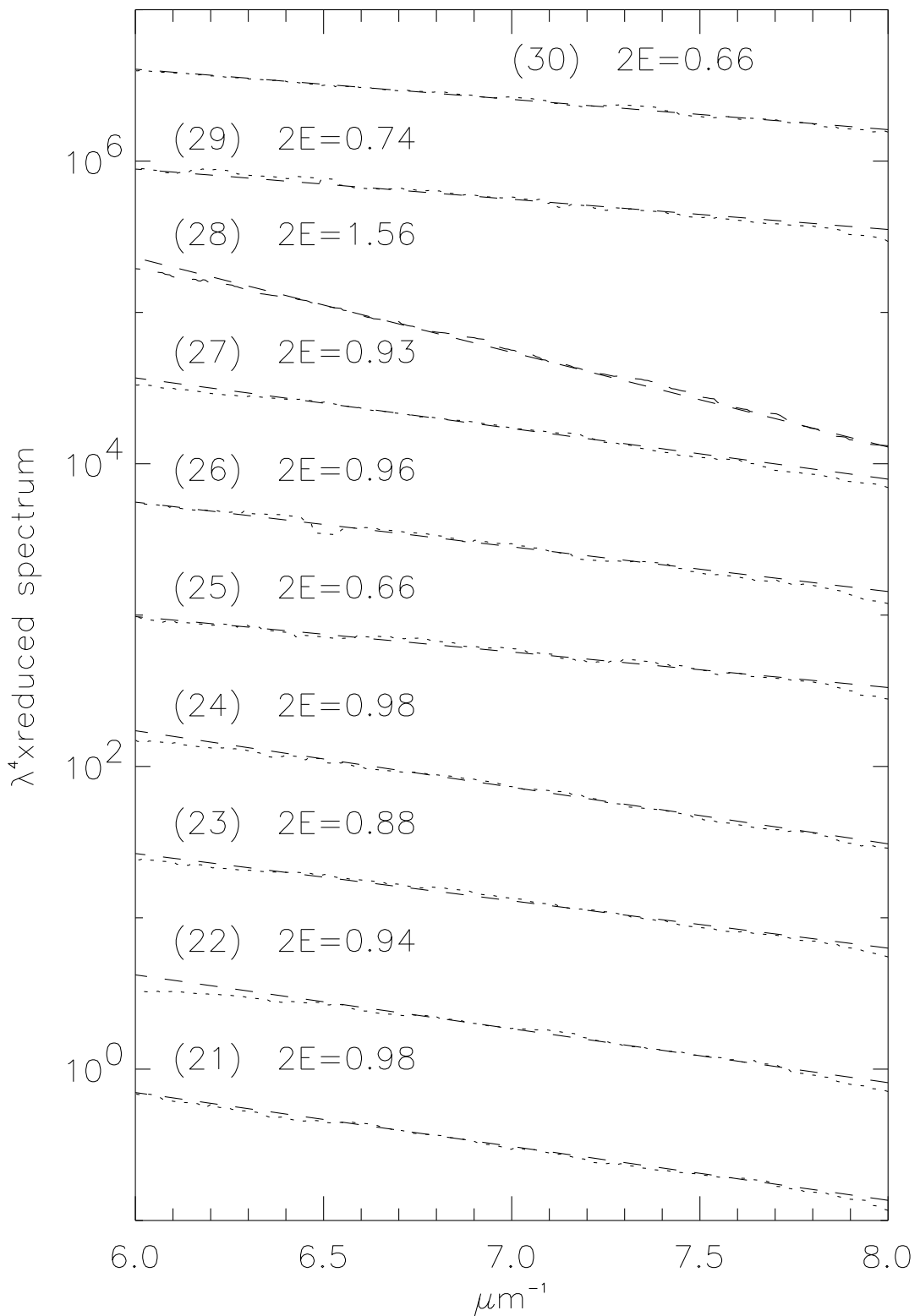


Fig. 1. Far-UV reduced spectra of the reddened stars multiplied by  $\lambda^4$ . The number above each curve corresponds to the star number, first column of Table 1.

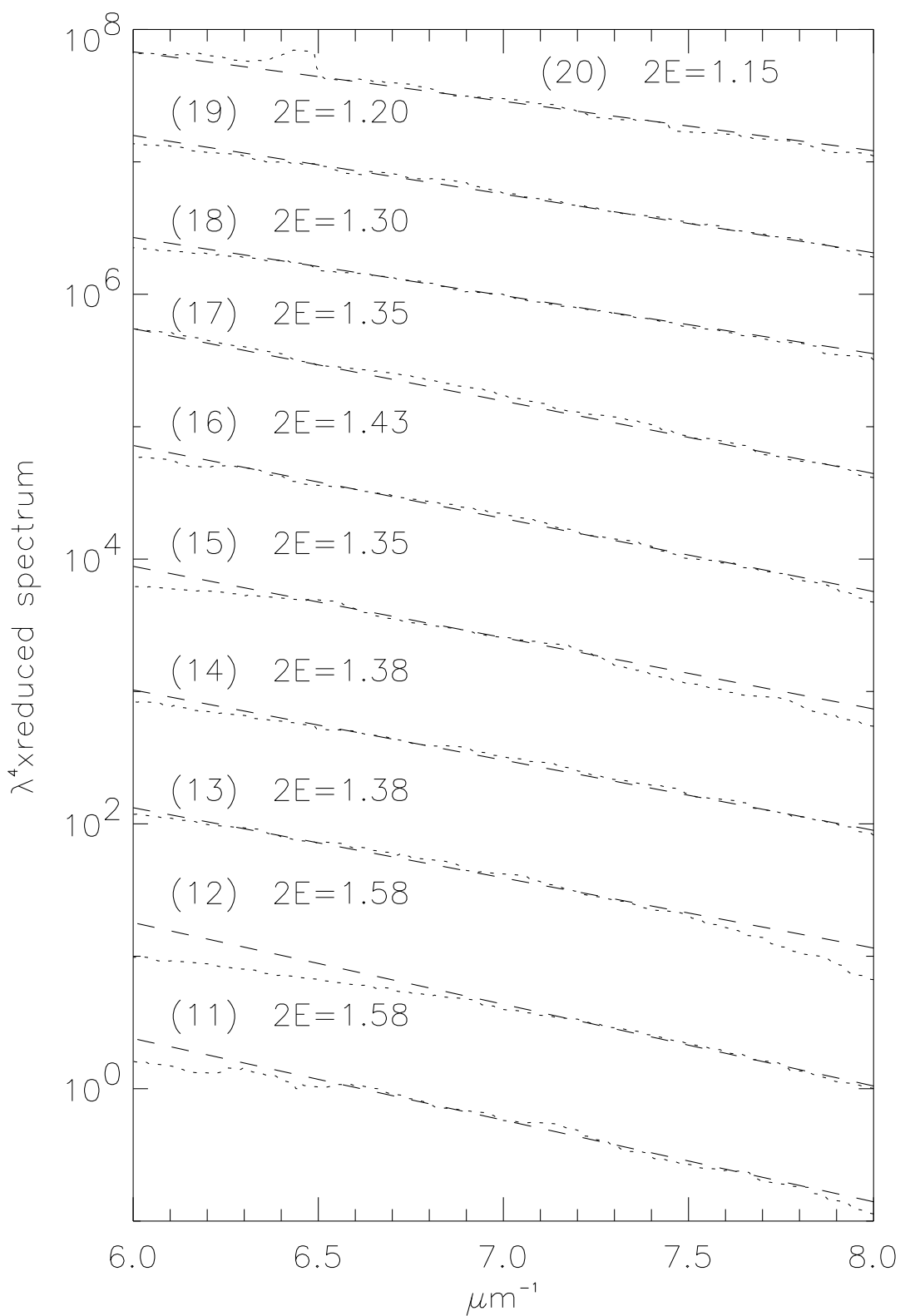


Fig. 2. Figure 1 continued.

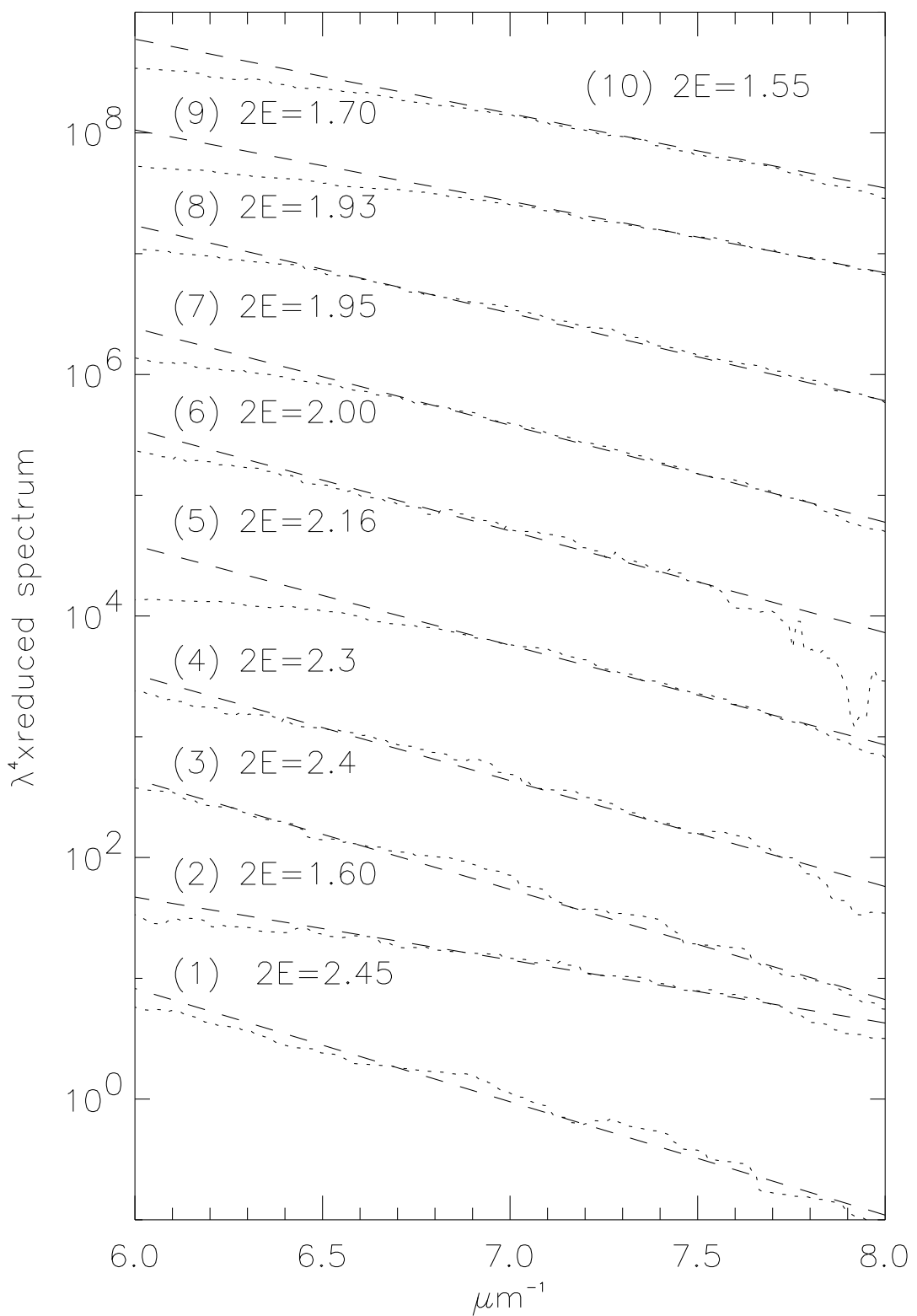


Fig. 3. Figure 1 continued.

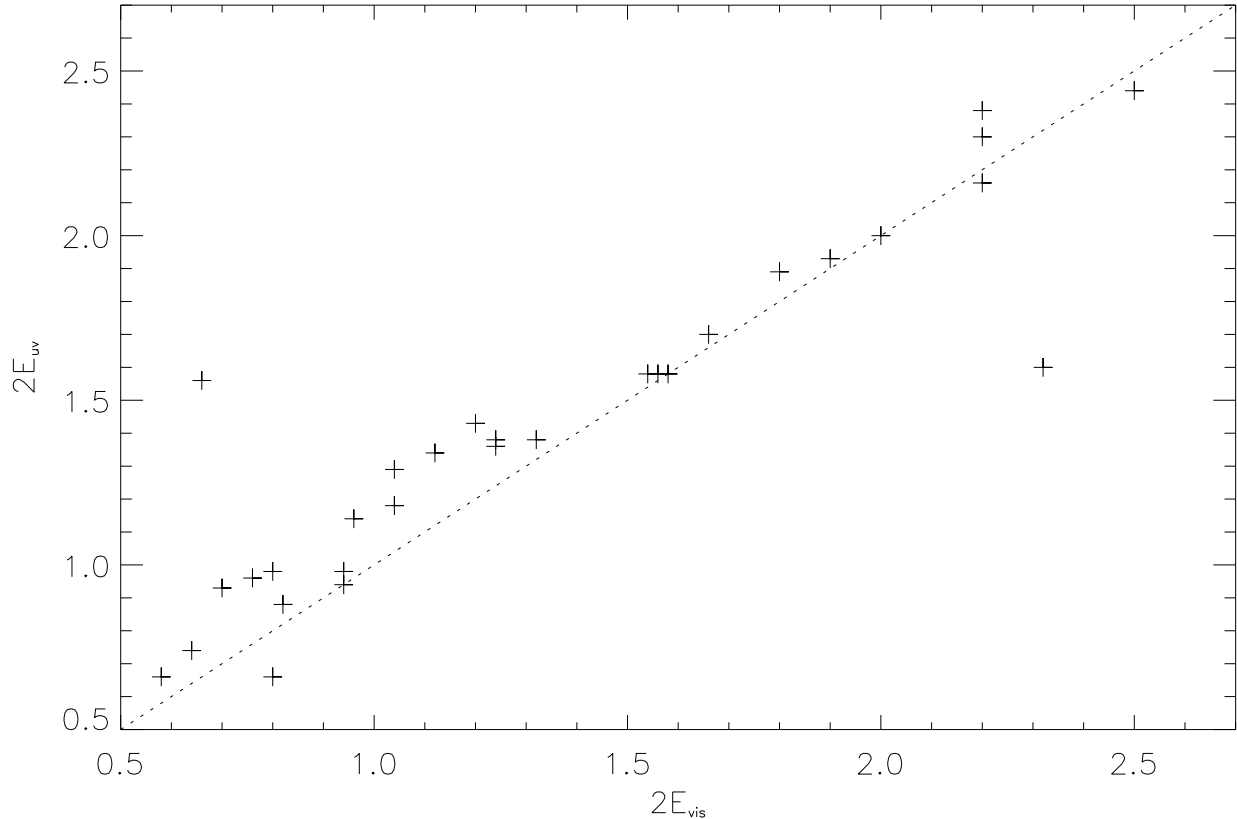


Fig. 4. Plot of  $2E_{uv}$  versus  $2E_{vis}$ .

- $E_{uv}$  and  $E_{vis}$  are correlated and have close values.
- There is a tendency for  $E_{uv}$  to be larger than  $E_{vis}$ .

This is true for all stars except for HD62542 and HD229196.

Even if the wavelength interval over which  $E_{uv}$  is determined is short -because of the 2200 Å on the one hand and the Ly $\alpha$  line on the other hand- the strong correlation between  $E_{uv}$  and  $E(B - V)$  (approximated by  $E_{vis}$ ) is remarkable enough not to be due to hazard. It implies a link between far-UV and visible extinctions.

On IRAS infrared images (see also the Palomar images and Cardelli & Savage (1988)), HD62542 is close to the edge of a bow-like structure, perhaps the front ridge of a shock wave. Interstellar matter associated to HD62542 may be the reason for the position of HD62542 on figure 4. Note that, according to Cardelli & Savage (1988), the properties of extinction in the direction of HD62542 and in the direction of HD29647 are very similar, while the position of HD29647 on the plot is on the  $x = y$  line.

## 4 Discussion

In the last thirty years, from the first publication of a large set of extinction curves by Bless & Savage (1972) and the later determination of an average and normalized extinction curve by Seaton (1979), there has been several attempts to find a link between far-UV extinction and  $E(B - V)$  (Savage et al., 1985; Fitzpatrick & Massa, 1988; Barbaro et al., 2001). Some conclusions, for instance the dependence of far-UV extinction on galactic longitude (why on galactic longitude?) which Witt et al. (1984) have claimed to observe, are probably dubious.

Important deviations from Seaton's curve in the far-UV, obvious through visual inspection, are commonly observed. The sample of stars used in this paper includes some of the directions which represent extreme cases of such deviations: HD147165 ( $\sigma$  Sco, Fig.1 of Savage (1975)), HD204827 (Savage et al., 1985; Fitzpatrick & Massa, 1988; Barbaro et al., 2001), HD29647 and HD62542 (Cardelli & Savage, 1988; Barbaro et al., 2001), HD37022 ( $\theta^1$  Ori, Cardelli & Clayton (1988); Barbaro et al. (2001)), HD169454, HD37367 (Barbaro et al., 2001).

These examples have been used as proof of independent variations of the three components of the extinction curve: visible and far-UV extinctions, and the 2200 Å bump region. If, as it is admitted in the standard theory of extinction, the light we receive from reddened stars is direct starlight alone, with no addition of scattered light, each of these components must be due to a specific class of interstellar grains, present in all directions, but in different proportions. This convenient way of solving the problem of interstellar extinction faces two major difficulties: there is up to now no satisfying identification of any of the three types of grains (except for the large grains responsible for the visible extinction, see Landgraf et al. (1999)) and, there does not seem to be any logic in the grain type repartition in relation to environment.

It is paradoxal to see how what should be a supplementary degree of freedom turns to heavy constraints on the grains' composition. Adjustment of the proportion of each type of grains permits to fit most individual extinction curves. Meanwhile, the specific extinction properties each type of grains must have, along with cosmic abundance limitations, impose heavy constraints on the grains' composition and on the evolution of dust from one environment to another (Li & Greenberg, 1997).

The mathematical decomposition of the extinction curve proposed by Fitzpatrick & Massa (1988) also fails to show a relation between far-UV and optical extinctions (Fitzpatrick & Massa, 1988; Barbaro et al., 2001). Fitzpatrick & Massa (1988) (section V, first paragraph) note that any attempt to

relate far-UV and optical extinctions strongly depends upon the adopted set of fitting functions. It is certain that within the standard theory framework and with the Fitzpatrick & Massa (1988) decomposition, which for the far-UV part of the spectrum has no physical basis at all, there was little chance to find a relation between the linear optical extinction and the far-UV extinction.

Conclusions of section 3 are a first step in the comprehension of the relation between the visible and the far-UV extinctions. The relation found between the slope of the extinction curve in these two wavelengths domains is expected if the spectra of reddened stars are contaminated by scattered light and if the linear visible extinction also applies to UV light. This relation exists even in the directions (mentioned in the first paragraph of this section) quoted to have a peculiar far-UV extinction.

## 5 Conclusion

I have used extinction curves in directions of sufficient reddening to show that far-UV and visible extinctions are related. In these directions, extinction is strong enough for direct starlight to be negligible in the far-UV; the far-UV light we receive is all scattered light. The far-UV reduced spectrum of the stars depends on  $\lambda$  as  $\lambda^{-n} e^{-2E(B-V)/\lambda}$  ( $\lambda$  in  $\mu\text{m}$ ,  $n = 4$ ).

Behind the apparent broad range of behavior so far found in the far-UV extinction curves (Bless & Savage, 1972), there is an underlying and simple order which relates far-UV extinction to visible reddening. Accepting this relation requires to question the standard interpretation of the UV extinction curve. It implies the abandonment of existing grain models, for which the extinction curve is the superimposition of the extinction curves of three separate kinds of grains. It also questions the existence of constituents of interstellar matter (PAH, HAC ...) which these models tried to prove using the extinction properties of interstellar dust at UV wavelengths.

The paper also gives credit to an idea I have tried to introduce in previous papers: the average extinction properties of interstellar dust are similar in most directions of space. Deeper understanding on the truth and limits of this proposal will be reached through the obtention and the comparison of precise extinction curves covering the whole optical to far-UV domain.

## References

Aiello S., et al., 1988, A&AS, 73, 195  
 Barbaro G., et al., 2001, A&A, 365, 157

Bless R.C., Savage B.D., 1972, *ApJ*, 171, 293  
Cardelli J.A., Clayton G.C., 1988, *AJ*, 95, 516  
Cardelli J.A., Savage B.D., 1988, *ApJ*, 325, 864  
Fitzpatrick E.L., Massa D., 1988, *ApJ*, 328, 734  
Fitzpatrick E.L., Massa D., 1990, *ApJ*, 72, 163  
Houk N., Catalogue of two dimentional spectral types for the HD stars, Vol. 2, Michigan Sky Survey, 1978  
Jackson J.D., 'Classical Electrodynamics', Second Edition, John Wiley & Sons, 1975  
Landgraf M., et al., 1999, *Science*, 286, 2319  
Li A., Greenberg J. M., 1997, *A&A*, 323, 566  
Nandy K., et al., 1975, *A&A*, 44, 195  
Savage B.D., 1975, *ApJ*, 199, 92  
Savage B.D., Massa D., Meade M., 1985, *ApJS*, 59, 397  
Seaton M.J., 1979, *MNRAS*, 187, 73  
Walkens C., et al., 1996, *A&A*, 314, L17  
Witt A.N., Bohlin R.C., Stecher T.P., 1984, *ApJ*, 279, 698  
Zagury, F., 2000, *NewA*, 4, 211  
Zagury, F., 2000, *NewA*, 5, 285  
Zagury, F., 2001, *NewA*, 6/7, 403  
Zagury, F., 2001, *NewA*, 6/7, 415  
Zagury, F., 2001, *NewA*, 6/8, 471

Table 1  
Reddened stars

n°	name	Sp. Type	B – V	2E <sub>vis</sub> <sup>(1)</sup>	2E <sub>uv</sub> <sup>(2)</sup>	Ref. (3)
1	HD169454	B1Ia	0.95	2.50	2.44 ± 0.30	11
2	HD229196	O5	0.84	2.32	1.60 ± 0.20	7
3	HD204827	B0V	0.80	2.20	2.38 ± 0.30	10
4	BD+66 1661	O9V	0.81	2.20	2.30 ± 0.30	4
5	HD147889	B2III/IV	0.84	2.20	2.16 ± 0.20	8
6	HD29647	B8III	0.91	2.00	2.00 ± 0.30	1
7	HD217061	B1V	0.68	1.90	1.93 ± 0.15	13
8	BD+62 2125	B1.5V	0.65	1.80	1.89 ± 0.20	11
9	HD216898	O8.5V/9V	0.53	1.66	1.70 ± 0.20	4
10	HD217463	B1.5Vn	0.54	1.58	1.58 ± 0.15	13
11	HD251204	B0V	0.48	1.56	1.58 ± 0.10	13
12	BD+62 2154	B1V	0.51	1.54	1.58 ± 0.10	13
13	HD239729	B0V	0.36	1.32	1.38 ± 0.20	10
14	HD161056	B1.5V	0.37	1.24	1.38 ± 0.10	13
15	HD200775	B2Ve	0.38	1.24	1.36 ± 0.10	8
16	HD217979	B1V	0.35	1.20	1.43 ± 0.15	13
17	HD21483	B3III	0.36	1.12	1.34 ± 0.20	9
18	HD12993	O6.5V/O5	0.20	1.04	1.29 ± 0.07	11
19	HD13338	B1V/B1III	0.26	1.04	1.18 ± 0.10	13
20	HD93250	O5/O7	0.16	0.96	1.14 ± 0.10	11
21	HD190944	B1.5Vne	0.22	0.94	0.98 ± 0.08	13
22	HD147933	B2V/B3V	0.23	0.94	0.94 ± 0.07	8
23	HD154445	B1V	0.15	0.82	0.88 ± 0.10	13
24	HD37367	B2IV/V	0.16	0.80	0.98 ± 0.08	8
25	HD147165	B1III	0.14	0.80	0.66 ± 0.05	2
26	HD93222	O7/8	0.07	0.76	0.96 ± 0.08	11
27	HD37903	B1.5V	0.10	0.70	0.93 ± 0.10	13
28	HD62542	B5V	0.17	0.66	1.56 ± 0.10	3
29	HD37022	O6pe/O7V	0.00	0.64	0.74 ± 0.05	11
30	HD38087	B5V	0.12	0.58	0.66 ± 0.05	3

1 2E(B – V) deduced from B – V and from the spectral type of the star.

2 2E(B – V) deduced from the UV spectrum of the star.

Table 2  
Unreddened stars

n°	name	Sp. Type	$E(B - V)$
1	HD10205	B8III	0.00
2	HD118716	B1III	0.03
3	HD199081	B5V	0.03
4	HD214680	O9V	0.10
5	HD215573	B6IV	0.00
6	HD222661	B9V	0.04
7	HD269698	O5e	0.10
8	HD31726	B2V	0.03
9	HD32630	B3V	0.02
10	HD36512	B0V	0.04
11	HD47839	O7V	0.07
12	HD58050	B2Ve	0.05
13	HD74273	B1.5V	0.04